

Investigating Synthesis of $\text{Cu}_2\text{ZnSn}(\text{Se}_{1-x},\text{S}_x)_4$ For Values of $0 \leq x \leq 1$ By S for Se Substitution, and Direct Sulphidisation of Metallic Precursors

Matthew Moynihan, Guillaume Zoppi, Robert Miles and Ian Forbes

Northumbria Photovoltaic Applications Centre, Northumbria University, Ellison Building, Newcastle-upon-Tyne, NE1 8ST, UK

Corresponding Author: matthew.moynihan@northumbria.ac.uk

Abstract

Thin layers of $\text{Cu}_2\text{ZnSn}(\text{Se}_{1-x},\text{S}_x)_4$ were produced by selenisation and subsequent sulphur substitution of DC sputter-deposited metallic CZT precursors on soda-lime glass. Values of $x=(0, 0.07, 0.12, 0.17, 0.28, 1)$ were measured by EDS. Samples were characterised optically and analysed using the Kubelka-Munk function, and found to have $0.96\text{eV} \leq E_g \leq 1.47\text{eV}$, varying approximately linearly with x . Samples underwent X-ray diffraction characterisation and substituted samples were found to comprise of multiple phase kesterite material with different levels of S substitution, averaging to the values obtained by EDS. The spectra were found to conform to Vegard's law, as peak location shifted linearly between $x=0$ and $x=1$. Binary phases are suspected to exist, because of some unusual behaviour at the location of the (200) peak. Lattice parameters for all phases were calculated and found to vary linearly between ($a=b=5.692$, $c=11.338$) for $x=0$ and ($a=b= 5.393$, $c= 10.863$) for $x=1$, which are in excellent agreement with previously published figures.

Introduction

In the search for low-cost, high conversion efficiency absorbers for photovoltaic cells, the direct band gap chalcogenide compound with a kesterite structure, copper zinc tin sulphur-selenide (CZTSe/S) has come to the fore. CZTSe/S contains only relatively low-cost elements. This material represents a sustainable development of the highest performance thin-film material from the same adamantine multinary chalcogenide member, the chalcopyrite, copper indium (gallium) diselenide (CIGS), which contains increasingly rare and expensive indium and gallium species.

The aim of this work is to develop this material using processing techniques that will enable scalable manufacturing that will also contribute to economically competitive photovoltaic electricity.

The band gap of CZTS/Se has been reported to vary between 0.95eV ($x=0$) and 1.5eV ($x=1$)[1] by changing the S:(S+Se) ratio. The substitution of sulphur for selenium in the

structure increases the band gap. Potentially this will enable tailoring of the band gap, both as a single bandgap material and as one in which the absorber layer band gap varies with depth, thus enabling higher collection efficiencies and lower recombination rates (as in the case of CIGS and CIGSeS).

In this paper we report the production of CZTSe/S with various S:(S+Se) ratios, synthesised by selenisation of DC-sputtered metallic CZT precursors then subsequent substitution of varying amounts of Se with S. Pure sulphides were also produced by direct sulphidisation of metallic precursors. The paper presents variations of bandgap value with S:(S+Se) ratio together with associated changes observed in the crystal structure.

Experimental Details

Thin films of CZTSe/S were produced by two methods. Both methods started with metallic CZT precursors produced by DC-sputter deposition from high-purity (5N) bimetallic and elemental (Cu/Zn, Cu/Sn, Zn and Sn) targets, using a Kurt J Lesker deposition system, to produce slightly copper-poor and zinc-rich precursors $0.33\mu\text{m}$ thick. The composition was assessed using an FEI (Philips) Environmental Scanning Electron Microscope (ESEM) to perform energy dispersive x-ray spectroscopy (EDS) and determined to be 43% Cu, 32% Zn and 25% Sn (%at). Most precursors were evaporation-coated with Se using a Kurt J Lesker evaporation system, then heated in a rarefied Ar atmosphere to a temperature of 530°C as it has previously been reported in literature as optimal for the formation of CZTSe[2]. This produced completely converted selenides ($x=0$). These selenides were optically characterised for diffuse reflectance using an integrating sphere in a Shimadzu Solidspec3700 spectrophotometer; had their composition assessed using EDS; and the structural properties of the films and were studied by X-ray diffraction (XRD) using a Siemens D5000 diffractometer.

The characterised selenides, along with remaining as-deposited precursors, were subsequently annealed in closed graphite boxes with varying quantities of evaporation-

deposited sulphur in a rarefied atmosphere of forming gas (10% H₂/N₂) at temperatures of 530°C, to enable a substitution reaction to occur.

CZTSe/S samples were produced with values of $x=(0, 0.07, 0.12, 0.17, 0.28, 1)$, as measured by EDS. These samples were again optically characterised and analysed using the Kubelka-Munk method, SEM micrographs at 5000x magnification and XRD spectra were also taken and the XRD spectra computationally analysed to deconvolve overlapping peaks using 8th order pseudo-Voigt functions.

Results and Discussion

As expected, the absorption edge in CZTSe/S was found to vary dependent on the level of S for Se substitution. Figure 1 shows the shift in absorption edge for varying x ; we see that the absorption edge of CZTSe/S shifts roughly linearly towards that of CZTS with increasing levels of substitution.

The mid-points on each of the absorption edges shown in Figure 1 can be used to approximate the band gap of the sample. The spectra were also analysed using the Kubelka-Munk function (shown in Figure 2). The band gaps calculated by both methods are compared in Figure 3. It can be seen that using the absorption edge is a good approximation to the values obtained by the more accurate Kubelka-Munk method. Optical transmission spectra were also taken, but due to the thickness of the films (~1µm) and high absorption coefficient, the transmission spectra were not reliable enough to use for $(h\nu)^2$ vs $h\nu$ plots.

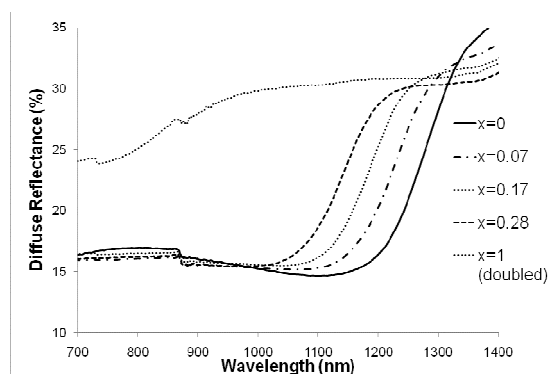


Figure 1 - Diffuse reflectance spectra for CZTSe/S samples of values of $0 \leq x \leq 1$. The values for the $x=1$ sample are doubled so that all data can be represented on one graph. The discontinuity at ~870nm is due to a change in diffraction grating in the spectrophotometer.

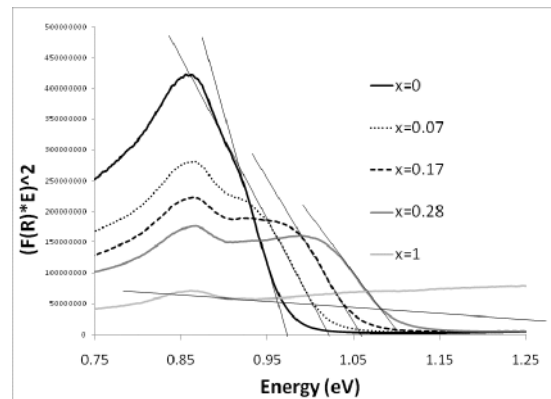


Figure 2 - Showing the curves obtained using the Kubelka-Munk method and the straight-line portions of the graphs used to calculate E_g . The point at which the extrapolated straight line crosses the x-axis shows the magnitude of the band gap of that sample.

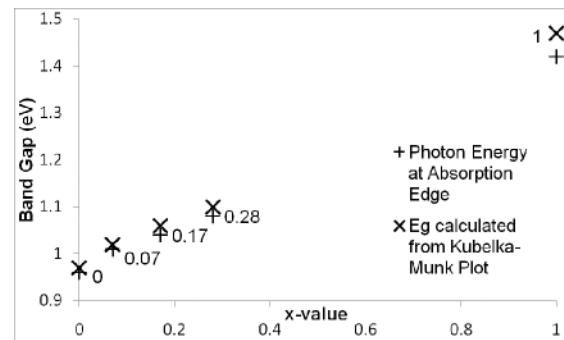


Figure 3 - absorption edge E_g values determined from Figure 1, compared to the values of E_g calculated using the Kubelka-Munk plots.

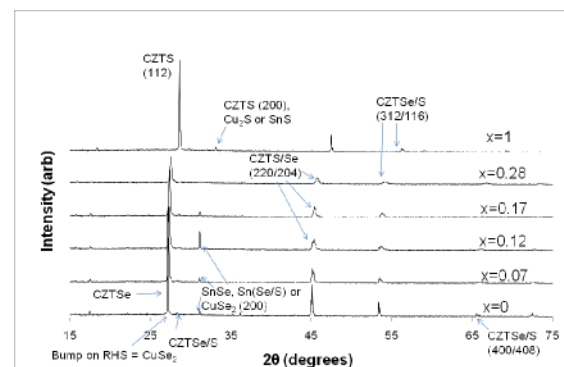


Figure 4 - Full-range XRD spectra of all samples between $x=0$ and $x=1$

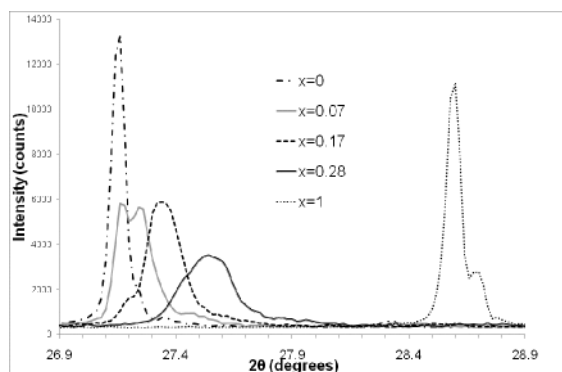


Figure 5 - X-ray diffraction spectra (detail) of samples of CZTSe/S with values of $0 \leq x \leq 1$, showing how the (112) peaks shift away from the CZTSe location towards the CZTS location as x increases.

The XRD spectra, presented in Figure 4 and the detail of the (112) peaks shown in Figure 5, show both peak-shifting and peak broadening with increasing level of substitution. The CZTSe ($x=0$) (112) and CZTS ($x=1$) (112) peaks on the left- and right-hand sides of Figure 5 respectively, show sharper, more defined peaks, compared to the sulpho-selenides. The broad peaks of the sulpho-selenides can be attributed to the overlapping peaks of a range of phases at different levels of substitution. Pseudo-Voigt analysis has confirmed this. The individual (112) peaks deconvolved in this analysis have been mapped in Figure 6.

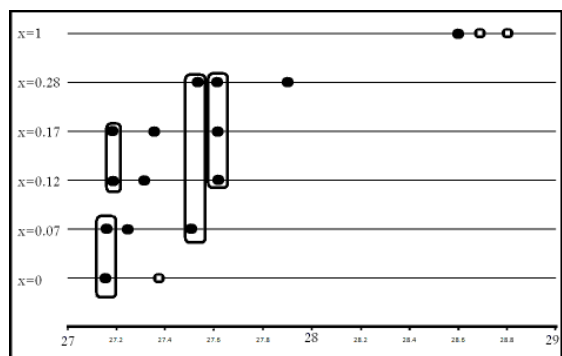


Figure 6 - Highlighting the positions of XRD peaks present in the spectra presented in Figure 5, locations determined by deconvolution using pseudo-Voigt formula. Peaks corresponding to phases that occur in more than one sample have been circled. Peaks corresponding to binary phases have white centres.

Using Vegard's law[3], we can calculate the compositions of the individual peaks present in the XRD spectra and see that each peak corresponds to a different level of substitution in the same kesterite structure, (some of the peaks can be attributed to binary phases – such as the right-hand peaks in the $x=0$ and

$x=1$ spectra (highlighted), which can be attributed to CuSe_2 and Cu_2S respectively.

From Figure 6, it is clear that single-phase sulpho-selenide material has not been produced. The data are consistent with a range of quinary phases with different levels of substitution having been formed, having a weighted average x -value equal to the value obtained via EDS. This range of phases would have a range of band gaps as well, which explains the shallow drop in diffuse reflectance (across $\sim 100\text{nm}$) visible in Figure 1.

This inhomogeneity of phases can be ascribed to the diffusion of sulphur from the front surface resulting in variations in the availability of sulphur during the substitution reaction, or to the particular stability of phases at certain values of x .

It is interesting to note that in each substitution reaction, 3 distinct phases are resolvable via deconvolution. The fact that some of these phases occur in more than one of the samples adds weight to the suggestion that there are certain stable arrangements of S and Se within the crystal lattice, and that individual grains are more likely to form with these levels of substitution or that as the diffusion edge moves through the sample a range of similar quinary phases will be produced in the diffusion gradient. It is also interesting to note that these substitutions resulted in unique intermediary phases between $x=0$ and $x=1$, rather than simply forming a mixture of CZTSe and CZTS. The fact that these intermediary phases have formed does show potential for accurately tailored band gaps in photovoltaic devices.

In Figure 4, we can see that as well as the (112) peaks shifting, the other CZTSe/S peaks move towards their respective CZTS counterparts with increasing levels of substitution, in agreement with Vegard's law. The peaks at 31.1 deg, however, do not shift noticeably. Peaks at this location could be ascribed to the (200) peaks of either CZTSe, CuSe_2 or $\text{Sn}(\text{Se}_n, \text{S}_{1-n})$ ($n=0.5, 1$).

Previous studies have found that in CZTSe where $\text{Cu}/(\text{Zn}+\text{Sn}) < 1.15$, the (200) peak is not found [4]. The samples used in this study have $\text{Cu}/(\text{Zn}+\text{Sn}) = 0.75$, so we can assume that the peak at 31.1deg is not CZTSe (200). Therefore either CuSe_2 or $\text{Sn}(\text{Se}_n, \text{S}_{1-n})$ (or possibly both) would be responsible for the peak at 31.1deg.

Both Cu_2S and SnS are located at 33.0° degrees and a corresponding double peak is labelled on the $x=1$ spectrum in *Figure 4*. It would be expected that these phases would also be subject to the substitution reaction, and following Vegard's law, we would expect these peaks to shift as well. It has been found, however, that both SnSe and the compound $\text{SnSe}_{0.5}\text{S}_{0.5}$ have peaks at 31.1° . Therefore, a possible explanation of the static peak is that it is caused by $\text{Sn}(\text{Se}_n, \text{S}_{1-n})$ and that this compound is only forming with values of $n=(0, 0.5)$ by substitution and $n=1$ in the pure sulphide. These samples are the subject of ongoing analysis to test this hypothesis.

The Bruker EVA software was used to calculate the lattice parameters for the CZTSe/S samples via cell tuning and peak matching, and it was found that $a=b$ varies between 5.393 and 5.692 ($x=1$ and $x=0$ respectively) and that c varies between 10.863 and 11.3375 ($x=1$ and $x=0$ respectively again). A tetragonal crystalline structure with $\alpha=\beta=\gamma=90^\circ$ and $a=b$ have been assumed. The intermediary phases were found to have values varying linearly with x between these two extremes, although the multiple phases present in each sample between $x=0.07$ and $x=0.28$ increased uncertainty in calculation of the lattice parameters for those samples. Where individual peaks were resolvable, sets of lattice parameters for each phase were calculated. The data is presented below.

x	a=b	c	a/c
0	5.692	11.338	1.992
0.07	5.692*	11.338*	1.992*
	5.674	11.300	1.991
0.12	5.674	11.271	1.986
	5.688	11.309	1.988
0.17	5.662	11.233	1.984
0.28	5.627	11.134	1.979
1	5.393	10.863	2.014

*Table 1 - Showing the lattice parameters for CZTSe/S samples with varying levels of sulphur. The values marked with * are the same as the values for $x=0$ because this phase is detected in both samples.*

This information shows us that the size of the unit cell decreases with increasing levels of substitution, and that the shape of the cell is altered slightly (a variation of about 1%).

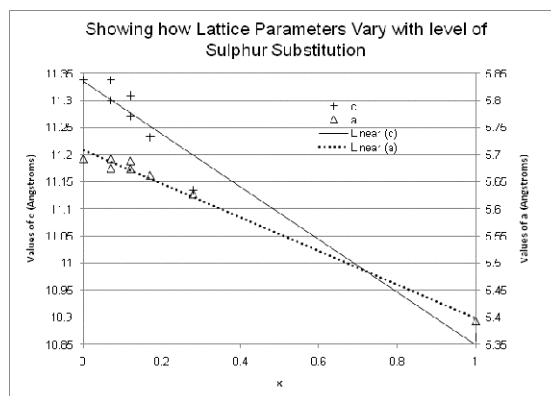


Figure 7 - Showing how lattice parameters of CZTSe/S vary with increasing values of x.

Conclusions

A range of copper zinc tin sulpho-selenide compounds have been produced by elemental sulphur substitution reactions with CZTSe synthesised from selenised DC-magnetron deposited metallic precursors. This processing offers a method of studying the evolution of the substitution process. It offers a promising route for tailoring the bandgap of absorber layers in thin film solar cells with the absence of toxic compounds such as H_2S , H_2Se or heavy metals, and without resorting to scarce and expensive metals such as indium and gallium. Bandgap values up to 1.1 eV were produced by substitution. However, at this stage the process is believed to result in a range of quinary kesterite phases with differing levels of substitution. The presence of stable structural configurations at certain values of x suggests that production of single phase sulpho-selenides is plausible, and the behaviour of the XRD spectra confirms that lattice parameters are similar enough for lattice matching between CZTSe/S phases not to be an issue. Overall, the work has shown that this is a possible route to high-efficiency, low cost photovoltaic absorbers.

References

- [1] Shiyu Chen et al. *App. Phys. Lett.* **94**, 041903 (2009)
- [2] S.M. Pawar et al. *Electrochimica Acta* Volume 55, Issue 12, (2010), Pp 4057-4061
- [3] A. R. Denton and N. W. Ashcroft, *Phys. Rev. A* 43, 3161–3164 (1991)
- [4] Babu et al. *Solar Energy Materials & Solar Cells* **94** 221–226 (2010)